Cellular Oncology 32 (2010) 259–274
DOI 10.3233/CLO-2010-0515
IOS Press

A peptide antagonist of the ErbB1 receptor inhibits receptor activation, tumor cell growth and migration *in vitro* and xenograft tumor growth *in vivo*

Ruodan Xu [a,b,*], Gro Klitgaard Povlsen [a,b,*], Vladislav Soroka [a], Elisabeth Bock [a] and Vladimir Berezin [a,**]

[a] *Protein Laboratory, Department of Neuroscience and Pharmacology, University of Copenhagen, Copenhagen, Denmark*

[b] *ENKAM Pharmaceuticals A/S, Copenhagen, Denmark*

Abstract. The epidermal growth factor family of receptor tyrosine kinases (ErbBs) plays essential roles in tumorigenesis and cancer disease progression, and therefore has become an attractive target for structure-based drug design. ErbB receptors are activated by ligand-induced homo- and heterodimerization. Structural studies have revealed that ErbB receptor dimers are stabilized by receptor–receptor interactions, primarily mediated by a region in the second extracellular domain, termed the "dimerization arm". The present study is the first biological characterization of a peptide, termed Inherbin3, which constitutes part of the dimerization arm of ErbB3. Inherbin3 binds to the extracellular domains of all four ErbB receptors, with the lowest peptide binding affinity for ErbB4. Inherbin3 functions as an antagonist of epidermal growth factor (EGF)-ErbB1 signaling. We show that Inherbin3 inhibits EGF-induced ErbB1 phosphorylation, cell growth, and migration in two human tumor cell lines, A549 and HN5, expressing moderate and high ErbB1 levels, respectively. Furthermore, we show that Inherbin3 inhibits tumor growth *in vivo* and induces apoptosis in a tumor xenograft model employing the human non-small cell lung cancer cell line A549. The Inherbin3 peptide may be a useful tool for investigating the mechanisms of ErbB receptor homo- and heterodimerization. Moreover, the here described biological effects of Inherbin3 suggest that peptide-based targeting of ErbB receptor dimerization is a promising anti-cancer therapeutic strategy.

Keywords: ErbB receptor, peptide mimetics, tumor cell proliferation and migration, tumor growth, apoptosis

Abbreviations

EGF	Epidermal growth factor;
TGFα	Transforming growth factor-α;
SPR	Surface plasmon resonance;
RU	Resonance units;
HER	Human epidermal growth factor receptor;
NSCLC	Non-small cell lung cancer;
SCCHN	Squamous cell carcinoma of the head and neck.

1. Introduction

The ErbB receptor tyrosine kinase family (also termed the human epidermal growth factor receptor [HER] family) consists of four members, termed ErbB1–4 or HER1–4, that share the same overall structure. They have a ligand-binding ectodomain composed of two leucine-rich domains (termed domain I and III, respectively) and two cysteine-rich domains (termed domain II and IV, respectively), a transmembrane domain, a short juxtamembrane section, a tyrosine kinase domain, and a tyrosine-containing C-terminal tail. ErbB1, ErbB3 and ErbB4 all bind different subsets of the large family of ErbB ligands, characterized by the presence of an epidermal growth factor (EGF)-like domain [20]. ErbB2 and ErbB3 are atypical

[*] These authors contributed equally to the work presented in this paper.

[**] Corresponding author: Vladimir Berezin, Protein Laboratory, Department of Neuroscience and Pharmacology, University of Copenhagen, Copenhagen, Denmark. E-mail: berezin@sund.ku.dk.

members of the family because ErbB2 lacks the ability to bind any extracellular ligand, whereas ErbB3 has a defective intracellular kinase domain [13,17].

Dimerization is essential for ErbB receptor activity because ErbB receptors are active only as homo- or heterodimers. At least 8 of 10 possible dimeric ErbB receptor combinations have been identified in living cells [32,40], and these combinations appear to be hierarchically organized, with ErbB2 as the preferred heterodimerization partner for the other ErbB receptors [14,19].

Solution of the crystal structures of the extracellular part of ErbB1 in complex with EGF [28] and transforming growth factor-α (TGFα) [11], respectively, contributed significantly to the understanding of the mechanisms of ErbB receptor dimerization [5,9,15]. Quite unexpectedly, these structures revealed that formation of ligand-binding ErbB1 homodimers is mediated solely by receptor–receptor interactions. Specifically, a prominent 20 amino acid loop, forming a β-hairpin, protrudes from domain II in each of the two ErbB1 molecules in the dimer and forms the main receptor–receptor interface, for which reason the loop has been termed the "dimerization arm" [11,28,31]. The essential role of the dimerization arm in ErbB1 dimerization and activation has been confirmed by several mutational studies [11,21,28,37]. Crystal structures of the extracellular parts of ErbB1, ErbB3 and ErbB4 in their inactive, ligand-free, monomeric form later revealed a dramatically different conformation, in which the β-hairpin loop of cystein-rich domain II interacts with domain IV and buries the dimerization arm, thereby preventing receptor dimerization [4, 6,10]. Structures of the EGFR ectodomain with EGF or TGFα demonstrate that binding of ligand to the leucine-rich domains I and III leads to a conformational change that exposes the dimerization loop and allows for interaction of receptor ectodomains [5,9, 15]. The dimerization arm sequence is highly conserved among the four ErbB receptor family members [31], and the dimerization arm is generally thought to play a similar role in all heterodimeric and homodimeric ErbB receptor complexes, although its importance only for the ErbB1 homodimer has been experimentally confirmed.

The involvement of ErbB receptors in tumorigenesis is well known. Their overexpression, mutation or dysregulation drives the development and progression of a variety of human cancers [27]. For example, ErbB1 is frequently overexpressed and/or mutated in non-small cell lung cancer (NSCLC), squamous cell carcinoma of the head and neck (SCCHN), colorectal cancer and pancreatic cancer [8]. Therefore, ErbB receptors represent important targets for anti-cancer drug design. In the last few years, several anti-ErbB drugs have been approved for clinical use against different cancers. These include monoclonal antibodies targeting different extracellular regions of ErbB1 or ErbB2 and small-molecule inhibitors of ErbB1 kinase activity. The use of small peptides capable of binding to specific regions in the extracellular part of one or several ErbB receptors, thereby interfering with the function of the receptors, represents an attractive alternative to antibody-based targeting of the extracellular parts of ErbB receptors. Recent attempts to develop peptide inhibitors of the ErbB receptors include peptides mimicking the complementarity-determining region of clinically active anti-ErbB antibodies (such as the Trastuzumab antibody) [3,30], antagonistic peptides with homology to ErbB receptor ligands [24], and peptides that target regions in domain IV thought to be important for ErbB receptor dimerization [2].

In the present study, we show that a peptide, termed Inherbin3, which constitutes part of the dimerization arm sequence of ErbB3, is able to bind to the extracellular domains of the ErbB receptors. At the cellular level, we show that this dimerization arm peptide functions as an antagonist of EGF-ErbB1 signaling. Specifically, Inherbin3 inhibits EGF-induced ErbB1 phosphorylation, growth and migration in human NSCLC A549 cells and human SCCHN HN5 cells, which express moderate and high ErbB1 levels, respectively. Furthermore, in two of three independently performed *in vivo* studies, Inherbin3 significantly inhibited the growth of A549 xenograft tumors and induced apoptosis of A549 cells in these tumors, which suggest that peptide-based targeting of the ErbB dimerization arm may be a promising novel therapeutic approach against ErbB expressing cancers.

2. Materials and methods

2.1. Peptides

All peptides were purchased from Schafer-N (Copenhagen, Denmark). Peptides were synthesized using the Fmoc-protection strategy on TentaGel resin (Rapp Polymere, Tübingen, Germany) using Fmoc-protected amino acids (Calbiochem-Novabiochem, San Diego, CA, USA). The Inherbin3 peptide from the human ErbB3 sequence (244-LVYNKLTFQLEPNPHTK-260;

UniProtKB/SwissProt No. P21860) was synthesized in two forms: (i) a dimeric peptide, termed Inherbin3, composed of two linear monomers linked together by a C-terminal lysine residue, and (ii) a tetrameric dendrimer, termed Inherbin3d, composed of four monomers coupled to a lysine backbone. The scrambled Inherbin3 peptide (KHKLPYNFNLETTVQPL) was only synthesized in the dimeric form and termed scr-Inherbin3. Peptides were at least 85% pure as estimated by high performance liquid chromatography (HPLC).

2.2. Recombinant proteins

The recombinant proteins comprising the Fc region of human IgG_1 and the Fc protein fused to the extracellular parts of human ErbB1, ErbB2, ErbB3 or ErbB4 were purchased from R&D Systems Europe (Abingdon, UK).

2.3. Antibodies and drugs

ErbB1 (cat #2232) and HER2/ErbB2 (cat #2165) were purchased from Cell Signaling Technology (Danvers, MA, USA). ErbB3 (cat sc-285) and ErbB4 (cat sc-283) were purchased from Santa Cruz Biotechnology (CA, USA). Taxol was from Bristol-Myers Squibb (Princeton, NJ, USA), Tarceva was from OSI Pharmaceuticals (Melville, NY, USA), and Cetuximab was from Merck KGaA (Darmstadt, Germany).

2.4. Cell lines

HN5 cells [18] were a generous gift from Dr. Nina Pedersen, Department of Radiation Biology, The Finsen Center, Copenhagen University Hospital, Copenhagen, Denmark. A549 cells and Cos-7 cells were purchased from ATCC (ATCC# CCl-185, CRL-1651). HN5, A549 and Cos-7 cells were grown in full growth medium: Dulbecco's Modified Eagle's Medium (DMEM; Substrate Department, Panum Institute, Copenhagen, Denmark) supplemented with 10% fetal calf serum (Invitrogen, Carlsbad, CA, USA), 1% penicillin–streptomycin (v/v; 10.000 units/ml and 10.000 µg/ml, respectively; Invitrogen) and 1% Glutamax (v/v; Invitrogen).

2.5. Binding analysis

Real-time biomolecular interaction analysis was performed employing the surface plasmon resonance (SPR) instrument BIAcore-2000 (GE Healthcare, Uppsala, Sweden) at 25°C using ready-made HBS-EP buffer (10 mM Hepes, pH 7.4, 150 mM NaCl, 3 mM EDTA, 0.005% surfactant P20; GE Healthcare) as running buffer. Peptides were immobilized non-covalently on the surface of a CM5 sensor chip (GE Healthcare) by electrostatic preconcentration using an amine-coupling procedure according to the manufacturer's instructions. 7000–9000 resonance units (RU) of peptide were immobilized on the chip. A reference surface was generated simultaneously under the same conditions but without peptide injection and used as a blank chip control. ErbB receptor proteins were injected at various concentrations at a flow rate of 20 µl/min, and binding to the peptides immobilized on the chip was measured in real-time. After each binding cycle, the sensor chip was regenerated by three injections of 50 mM NaOH. The curve corresponding to the difference between signals on flow cells with immobilized peptide and the signal on the blank flow cell was used for analysis. Data were analyzed by non-linear curve fitting using BIAevaluation software (GE Healthcare). Three independent experiments were performed.

2.6. ErbB expression profile in two ErbB1-overexpressing human tumor cell lines

2×10^6 cells (HN5 or A549) were grown in 6 cm dishes. Lysates of HN5 and A549 cells were subjected to SDS-PAGE electrophoresis followed by immunoblotting using antibodies against ErbB1 (1:1000), ErbB2 (1:1000), ErbB3 (1:1000) and ErbB4 (1:1000). In each experiment, the same amount of protein was used, and the experiments were repeated independently 2 times.

2.7. ErbB receptor phosphorylation

2×10^6 cells (HN5 or A549) were grown in 6 cm dishes, treated with peptide at the indicated concentrations for 30 min, and then stimulated with 10 ng/ml EGF for 5 min. The cultures were rinsed twice with sterile phosphate-buffered saline (PBS), then lysed directly with ice-cold lysis buffer containing 1% (v/v) NP-40 (Sigma-Aldrich, Copenhagen, Denmark), phosphatase inhibitors (1:100; Phosphatase Inhibitor Cocktail II; Calbiochem, La Jolla, CA, USA),

and protease inhibitors (1:50; Complete™ Protease Inhibitor Cocktail; Boehringer Mannheim Biochemica, Mannheim, Germany). Cells were lysed for 30 min and then spun for 20 min at 20,000 × *g* at 4°C. Protein concentrations were determined using the BCA Protein Assay Kit (Thermo Scientific, Rockford, IL, USA). Cleared lysate samples containing 500 µg total protein were incubated with 15 µl agarose-coupled anti-phosphotyrosine antibodies (4G10-AC; Upstate Biotechnologies, Lake Placid, NY, USA) and PBS overnight at 4°C. The bound proteins were washed and eluted with 180 mM phenylphosphate (Sigma-Aldrich). SDS-sample buffer was added to purified samples (20 µl from each sample) and boiled for 5 min. Samples were separated by 8% NuPAGE Tris-Glycine gels (Invitrogen) and transferred to a polyvinylidene fluoride membrane (Millipore, Bedford, MA, USA). Membranes were blocked for non-specific binding with 5% (w/v) non-fat dry milk at room temperature for 1 h and incubated with primary polyclonal rabbit antibodies against ErbB1 (1:1000) for 2 h at room temperature or overnight at 4°C. Horseradish peroxidase-conjugated swine anti-rabbit IgG secondary antibodies (1:1000; DakoCytomation, Glostrup, Denmark) were applied for 1 h at room temperature. The immune complexes were developed by SuperSignal® West Dura extended duration substrate (Pierce, Rockford, IL, USA) and visualized and quantified using SynGene Gene Tool image analysis software (Synoptics Ltd., Cambridge, UK). In each experiment, the same amount of protein was used for purification, and the experiments were repeated independently at least four times.

2.8. Cell growth (MTS staining)

Cells (HN5, A549 or Cos-7) were seeded at 2×10^3 cells per well in 96-well plates in full growth medium (see above) or starvation medium (as full growth medium but without serum) to allow cells to adhere. After 12 h of incubation, the cells were treated with peptides, Cetuximab (Erbitux, Merck Ltd., Middlesex, UK) or the ErbB1 kinase inhibitor PD153035 (Calbiochem, Merck Ltd., Nottingham, UK) at concentrations indicated in the figures. Plates were returned to the incubator for 72 h. One hour prior to reading the plates, MTS One Solution Reagent (Promega, Madison, WI, USA) was added under sterile conditions, and the cells were returned to the incubator. After the incubation, the plates were read in an enzyme-linked immunosorbent assay (ELISA) plate reader by absorbance measurements at 490 nm. Each experiment was performed in six replicate wells and independently repeated four times.

2.9. Cell migration assay

Cell migration was examined with the use of a QCM™ Chemotaxis 96-well 8 µm Migration Kit (Chemicon, Millipore, Billerica, MA, USA). 5×10^4 cells per well were seeded in the migration chamber (upper tray) in starvation medium. The feeder chamber (lower tray) was filled with full growth medium (see above), with the exception of the first row, which was filled with starvation medium (serving as the "no serum" control). Peptide, inhibitors or vehicle (MilliQ water) was added to all wells in the upper and lower tray at the concentrations indicated in the figures. The chambers were incubated for 24 h in a 37°C incubator with 5% CO_2. After the incubation, cells that had migrated through the membrane were assessed by means of fluorescent CyQuant GR Dye following the manufacturer's instructions. Each experiment was performed in six replicate wells and repeated four times.

2.10. Animals

Six- to 7-week-old female immunodeficient SCID mice ($CB17^{-/-}$, Taconic Farms, Ejby, Denmark) weighing 15–20 g were housed in plastic cages supplied with filtertops, had free access to standard laboratory food and water, and were kept at 22°C under a 12 h light/dark cycle.

2.11. In vivo tumor growth

Tumors were induced in female immunodeficient SCID mice by inoculating 5×10^6 A549 cells subcutaneously in the lower left flank of the animals. Animals were divided into treatment groups, with 8–10 animals per group, when the tumors reached a size of 50–100 mm^3 (on day 6 after tumor inoculation). Animals were allocated according to their tumor volume and body weight so that the average tumor volume and body weight of all groups were as similar as possible. Treatment with Inherbin3, scr-Inherbin3, vehicle (sterile water or MilliQ Water), Taxol, Tarceva and Cetuximab was initiated on the day following group allocation (day 7 after tumor inoculation) separately in three independent experiments. Inherbin3, scr-Inherbin3 or vehicle was administered subcutaneously daily in a volume of 100 µl per animal. Taxol was administered intraperitoneally three times weekly, and Cetuximab was administered intraperitoneally twice weekly in a volume of 100 µl per animal. Tarceva was administered orally three times weekly in a volume of 100 µl per ani-

mal. Tumor volumes were assessed three times weekly by direct measurement using a digital caliper and calculated using the formula: (larger diameter) × (smaller diameter)$^2/2$. All tumor reads were done by personel blinded towards the treatment groups of the animals.

2.12. TUNEL assay

On day 40, tumor-bearing mice were sacrificed by cervical dislocation and the primary tumors were separated from the surrounding muscles. The tumors were fixed in formalin to perform paraffin-embedded sections for a morphological study. Blocks containing the tumor tissues were embedded in paraffin and sliced with a microtome at 10 μm thickness. Analysis of apoptotic cells was performed using a commercially available FragEL™ DNA Fragmentation Detection Kit (Calbiochem, Nottingham, UK). For terminal transferase reactions (TUNEL), the procedure was performed according to the manufacturer's instructions. Briefly, three 10 μm-thick sections of each tumor were placed on one slide, and after deparaffinization and rehydration, the sections were treated with proteinase K (20 μm/ml in 10 mM Tris/Hcl, pH 7.4) for 30 min at 37°C. This was followed by washings with tris-buffered saline and incubation with TdT (terminal deoxynucleotidyl transferase) reaction mixture containing the Biotin labeling reagent and the enzyme reagent in a humidified chamber at 37°C for 90 min. The specimens were then incubated with streptavidin–horseradish peroxidase (HRP) conjugate at room temperature for 30 min. Negative controls were not treated with the TdT solution. The presence of clear nuclear staining was indicative of apoptotic cells. The number of TUNEL-positive tumor cell nuclei was counted. To quantify the apoptotic cells, the TUNEL-positive cells were counted in 10 random fields at 40× magnification.

3. Results

3.1. The Inherbin3 peptide binds to ErbB1 and ErbB3 and with lower affinity to ErbB2 and ErbB4

On the basis of the sequences and crystal structures of the extracellular parts of the ErbB receptors [4,6, 7,10–12,28,31], we designed a series of peptides derived from the dimerization arm region of ErbB receptors [31]. Figure 1A shows a backbone diagram of the crystal structure of a homodimer of the extracellular parts of two ErbB1 molecules (in green and blue, respectively) in complex with EGF (in red), in which the dimerization arms of the two ErbB1 modules are marked in yellow and cyan, respectively (PDB:1IVO). Figure 1B shows a homology alignment of the dimerization arm sequences from human ErbB1–4 (SwissProt No. P00533, P04626, P21860 and Q9UJM3, respectively).

Upon binding of relevant ligands, the ErbB receptors are able to engage in almost all theoretically possible homo- and heterodimeric ErbB combinations [32, 40], and the dimerization arm is highly likely to be involved in the formation of the receptor–receptor interface in all of these homo- and heterodimers, although this hypothesis remains to be directly experimentally confirmed. This suggests that the dimerization arm from any given ErbB receptor will be able to bind to any of the other ErbB receptor family members. To test this hypothesis, we synthesized four peptides encompassing a strand-loop-strand region of the dimerization arms of ErbB1–4, termed Inherbin1–4, respectively (marked by arrows in Fig. 1B). Inherbin1, Inherbin2 and Inherbin4 were unstable, possibly because they contain methionine residues rendering peptide instability [34]. We decided to focus, therefore, on characterization of the biological effects of the Inherbin3 peptide.

First, we determined the ability of Inherbin3 to bind to the extracellular parts of the four ErbB receptors by means of SPR analysis (Fig. 2). The Inherbin3 peptide was synthesized as a tetrameric dendrimer, termed Inherbin3d, composed of four monomeric peptide chains coupled by their C-terminal ends to a lysine backbone, and this peptide was immobilized on the surface of a sensor chip. The use of the dendrimeric Inherbin3d peptide instead of the monomeric version allows for more flexibility of the immobilized peptide, minimizing the risk that the ErbB receptor binding sites in Inherbin3 will be masked upon immobilization of the peptide on the sensor chip surface. To assess the binding of the ErbB receptors, we employed commercially available recombinant chimeric proteins comprising the extracellular parts of ErbB1–4 fused to the Fc part of human IgG. Inherbin3 was derived from the dimerization arm of the ErbB3 receptor. Therefore we first tested the binding of ErbB3 to the immobilized peptide and found that it strongly bound to this receptor (Fig. 2A). Inherbin3 also bound to other ErbB receptors, ErbB1, ErbB2 and ErbB4, whereas no binding of the Fc protein alone was detected (Fig. 2B).

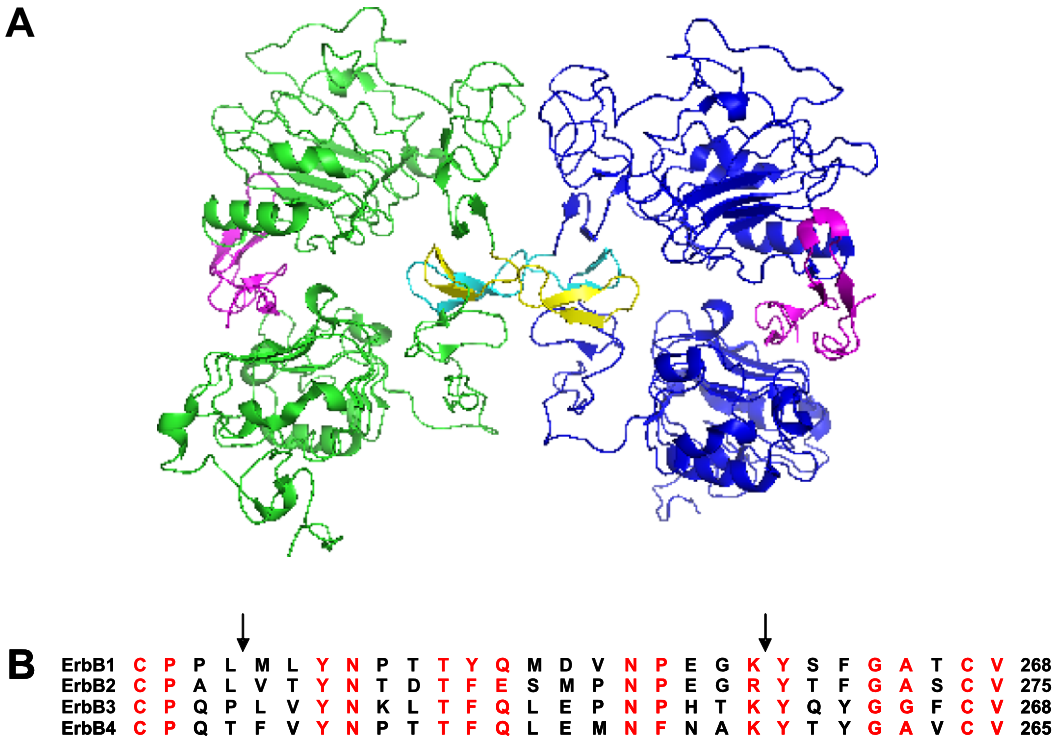

Fig. 1. The ErbB receptor dimerization arm motif. (A) Backbone diagram of the crystal structure of a homodimer of the first three extracellular domains of two human ErbB1 molecules (shown in green and blue, respectively), each complexed with one EGF molecule (marked in magenta) (PDB no. 1IVO). The "dimerization arms" of both ErbB1 molecules, constituting most of the receptor–receptor interaction interface in the structure, are shown in yellow (for the molecule in green) and cyan (for the molecule in blue). (B) Sequence alignment of the fifth disulfide-bonded module (dimerization arm) in the second extracellular domain of ErbB1–4. The N- and C-termini of the Inherbin peptides are marked with arrows. Residues that are identical in at least three ErbB family members are marked in red. (The colors are visible in the online version of the article.)

The equilibrium binding levels for ErbB1, ErbB2 and ErbB4 were clearly significantly lower than the binding levels obtained for ErbB3 at the end of the injections. The calculated affinity and rate constants for interaction of the Inherbin3 peptide with the ErbB1–4 receptors are presented in Table 1, from which it can be seen that ErbB1, ErbB2 and ErbB3 bind to Inherbin3 with affinities that are considerably higher than the binding affinity of ErbB4. Because ErbB1 is important in human cancers, we decided to further investigate the effects of Inherbin3 on ErbB1 activity and function.

3.2. *Inherbin3 inhibits EGF-induced ErbB1 phosphorylation in two human ErbB1-expressing tumor cell lines*

To explore the ability of the Inherbin3 peptide to function as an inhibitor of ligand-induced ErbB1 dimerization and activation, we assessed the effect of Inherbin3 on EGF-induced ErbB1 phosphorylation in two human tumor cell lines. HN5 [18] is a human SCCHN cell line characterized by strong ErbB1 overexpression and no expression of the other three ErbB receptors (Fig. 3). A549 is a human NSCLC cell line that expresses a moderate level of ErbB1 and ErbB3 and does not express ErbB2 and ErbB4 (Fig. 3).

As shown in Fig. 4, Inherbin3 significantly inhibited EGF-induced ErbB1 phosphorylation in both of these tumor cell lines, with the strongest inhibitory effect in the A549 cell line. For comparison, the effect of the monoclonal anti-ErbB1 antibody Cetuximab on ErbB1 phosphorylation in the two cell lines was also assessed. In both cell lines, treatment with 50 μg/ml Cetuximab resulted in complete blockade of EGF-induced ErbB1 phosphorylation. In conclusion, the data in Fig. 4 indicate that Inherbin3 at the tested dose partially inhibited EGF-induced ErbB1 phosphorylation, whereas Cetuximab conferred complete blockade of EGF-induced EbB1 phosphorylation.

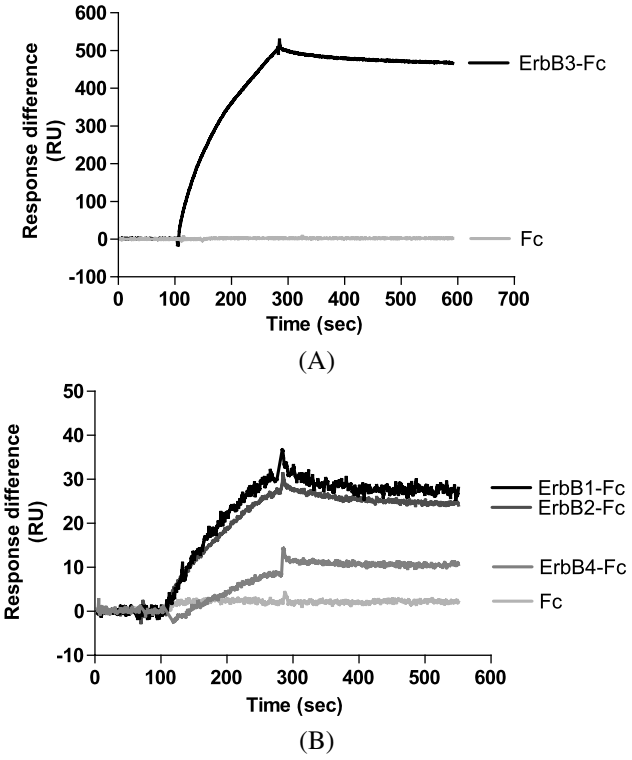

Fig. 2. Binding of ErbB receptors to Inherbin3. The Inherbin3 peptide was immobilized on the sensor chip, and recombinant chimeric proteins comprising the extracellular parts of the four ErbB receptors fused to the Fc part of human IgG were injected in concentration of 0.37 μM (ErbB2, ErbB3, ErbB4 and Fc alone) and 0.18 μM (ErbB1). Binding is expressed as the response difference between the binding to the sensor chip with the immobilized peptide and a blank sensor chip. (A) Binding of ErbB3–Fc and Fc to Inherbin3. (B) Binding of ErbB1–Fc, ErbB2–Fc and ErbB4–Fc, and Fc to Inherbin3.

Table 1
Affinity and rate constants for interaction of Inherbin3 with various ErbB receptors

ErbB receptors	Ka ($M^{-1}s^{-1}$)	Kd (s^{-1})	KD (M)
ErbB1–Fc	4.59×10^4	4.16×10^{-4}	9.06×10^{-9}
ErbB2–Fc	4.23×10^4	4.77×10^{-4}	1.13×10^{-8}
ErbB3–Fc	1.97×10^4	1.83×10^{-4}	9.29×10^{-9}
ErbB4–Fc	1.35×10^3	6.19×10^{-4}	4.59×10^{-7}

3.3. *Inherbin3 inhibits in vitro growth of ErbB1-expressing HN5 and A549 tumor cells but not ErbB-negative Cos-7 cells*

We next explored the ability of Inherbin3 to function as an inhibitor of HN5 and A549 cell growth *in vitro* via its inhibitory effect on ErbB1 activity. As shown in Fig. 5, Inherbin3 significantly and dose-dependently inhibited the growth of both cell lines but had no effect on the Cos-7 cell line, which expresses only a negligible amount of ErbB1 [35]. The inhibitory effect of Inherbin3 was most pronounced on HN5 cells (approximately 40% growth inhibition by the highest Inherbin3

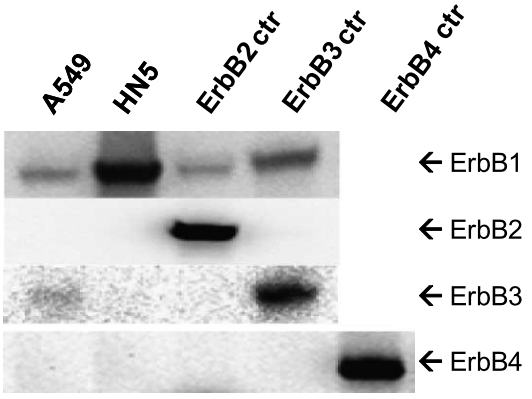

Fig. 3. ErbB expression profile in two ErbB1-overexpressing human tumor cell lines. Lysates of HN5 and A549 cells were subjected to SDS-PAGE electrophoresis followed by immunoblotting using antibodies against ErbB1–4. Lysates of cells expressing high amounts of individual ErbB receptors were used as positive controls (ErbB2 positive control: SKBR3 cells; ErbB3 positive control: MDA-MB-231 cells; ErbB4 positive control: HEK293 cells transfected with ErbB4 cDNA).

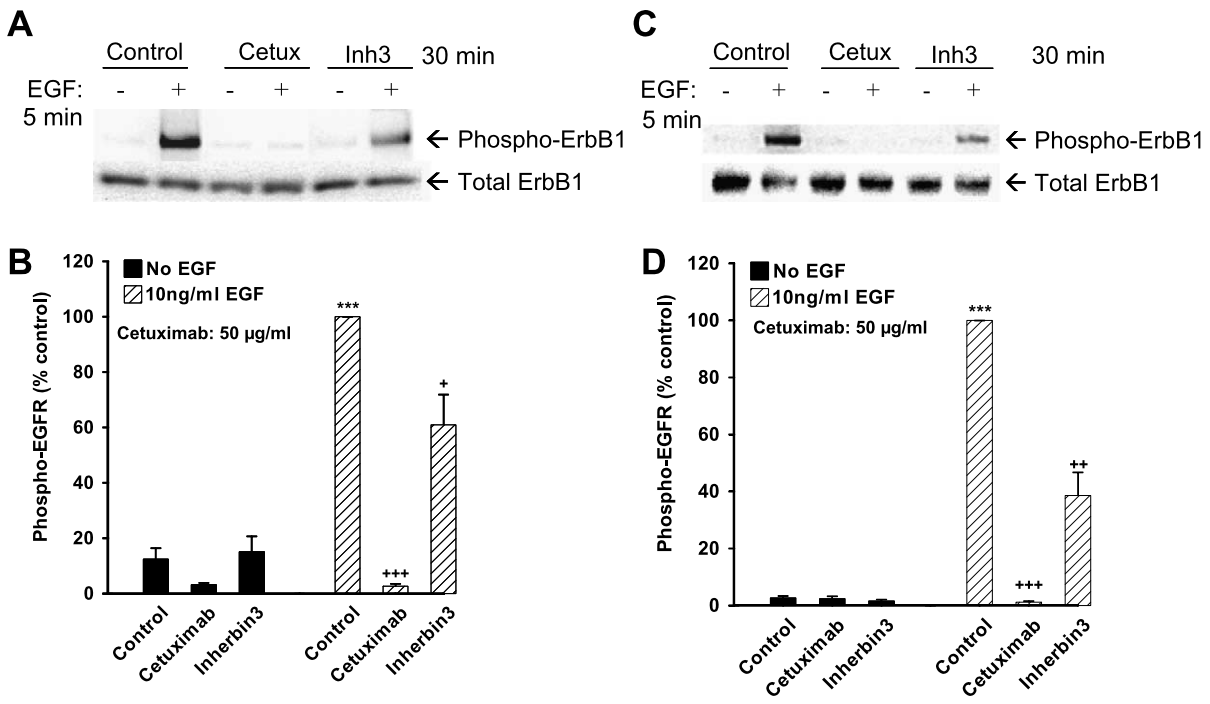

Fig. 4. Effect of Inherbin3 on ErbB1 phosphorylation. HN5 cells (A and B) or A549 cells (C and D) were treated with 23 µM Inherbin3 and 50 µg/ml Cetuximab for 30 min followed by stimulation with 10 ng/ml EGF for 5 min. For HN5 cells, immunoblotting was performed using phosphorylated ErbB1, followed by membrane stripping and reprobing against total ErbB1 and actin. For A549 cells, cell lysates were subjected to immunopurification using phospho-tyrosine antibodies followed by SDS-PAGE and blotting against total ErbB1. (A and C) Representative blots from one experiment. (B and D) Densitometric quantifications of phospho-ErbB1 immunoblots (B) or total ErbB1 blots of phosphotyrosine-purified lysates (D) from five to six independent experiments. The level of ErbB1 phosphorylation is expressed as mean ± SEM of band intensity in phospho-ErbB1 blots (B) or total ErbB1 blots of phosphotyrosine-purified lysates (D). The level of ErbB1 phosphorylation in EGF-treated cells not treated with peptide was set as 100%. $^{***}p < 0.001$, significant difference compared with untreated control cells (no peptide, no EGF) (Student's paired t-test). $^{+}p < 0.05$, $^{++}p < 0.001$, significant difference compared with EGF-treated control cells (no peptide, EGF) (Student's paired t-test).

dose tested) and rather small on A549 cells (approximately 20% growth inhibition by the highest Inherbin3 dose tested). In contrast, a scrambled Inherbin3 peptide, consisting of the same amino acids that constitute Inherbin3 but arranged in a randomly scrambled sequence, had no effect on A549 cell growth and only a slight (and not dose-dependent) effect on HN5 cell growth, indicating that the growth inhibitory effect of Inherbin3 is sequence-specific.

For comparison, the effects of the ErbB1-specific kinase inhibitor PD153035 and the anti-ErbB1 monoclonal antibody Cetuximab were assessed. PD153035 and Cetuximab strongly inhibited the HN5 cell growth, whereas these inhibitors had no significant effect on A549 cell growth. Thus, whereas Cetuximab and PD153035 have a stronger inhibitory effect than Inherbin3 in the ErbB1-overexpressing HN5 line, Inherbin3 has a stronger inhibitory effect than Cetuximab and PD153035 in the A549 cell line which expresses much lower amounts of ErbB1 (compared with HN5 cells), together with ErbB3 (which is not present in HN5 cells).

3.4. *Inherbin3 inhibits in vitro migration of HN5 and A549 tumor cells*

Apart from its role as a classic mitogenic signaling system, signaling via ErbB1 is known to stimulate cell motility and migration [38]. We therefore continued our characterization of the biological effects of Inherbin3 by investigating the effect of Inherbin3 on tumor cell migration. We employed the two tumor cell lines HN5 and A549, and cell migration was evaluated by means of a QCM Chemotaxis Migration Assay. Cells were seeded in starvation medium and allowed to migrate through a filter toward a chamber containing serum-supplemented medium (i.e., serum was used as chemoattractant) in the presence or ab-

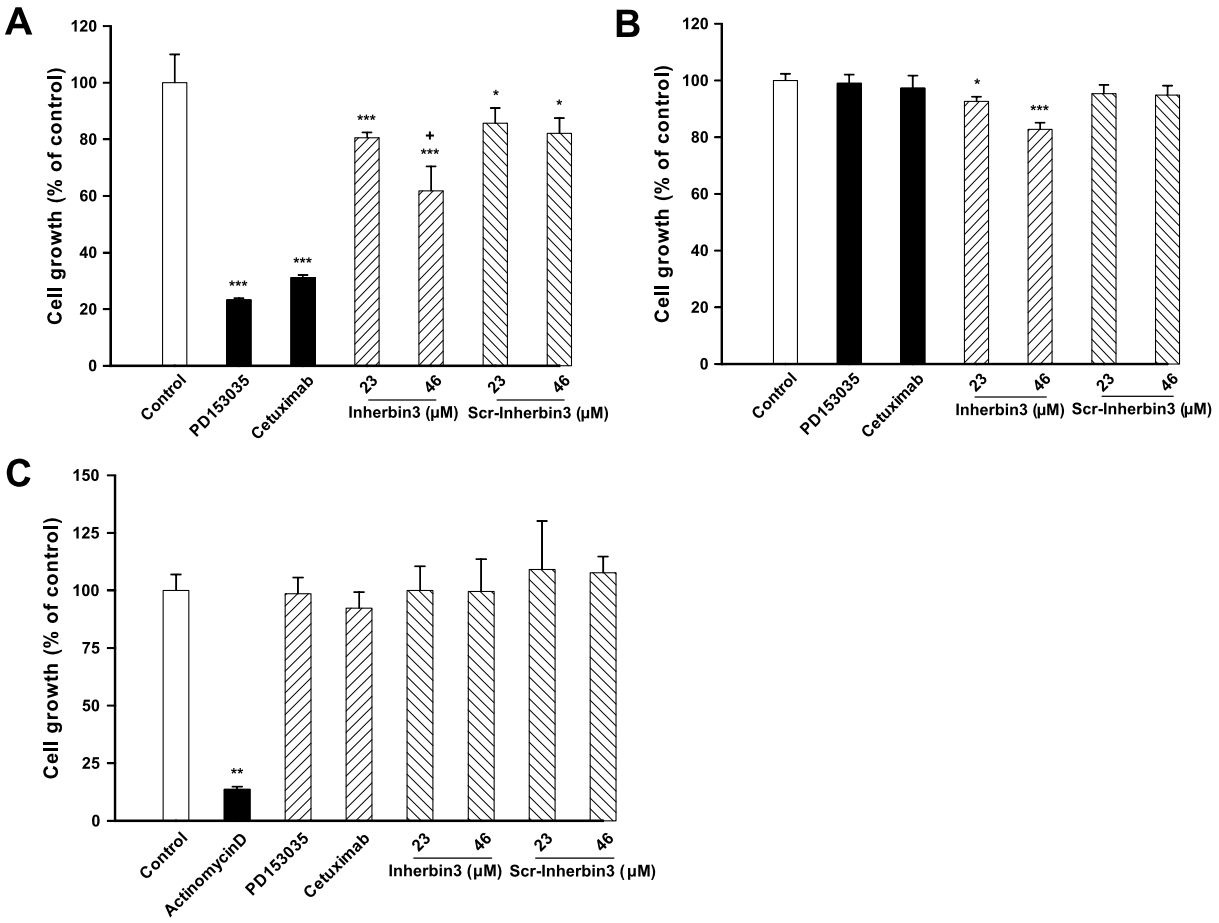

Fig. 5. Effect of Inherbin3 on *in vitro* cell growth of HN5 and A549 cells. HN5 cells (A), A549 cells (B) or Cos-7 cells (C) were seeded in full medium (containing 10% fetal calf serum) and treated with the indicated doses of Inherbin3, Scr-Inherbin3, 100 nM PD153035, or 50 μM Cetuximab. Cells were grown for 3 days, and cell growth was measured with MTS staining. Data are expressed as mean ± SEM of 6–8 independent experiments. $^{*}p < 0.05$, $^{**}p < 0.01$, $^{***}p < 0.001$, compared with untreated cells (control) (repeated-measures analysis of variance followed by Dunnett's *post hoc* test). $^{+}p < 0.05$, significant difference compared with Scr-Inherbin3 (46 μM) (Student's paired t-test).

sence of Inherbin3. As shown in Fig. 6, A549 cells showed a strong increase in cell migration when subjected to serum as chemoattractant, whereas HN5 cells showed the same basal migration rate regardless of whether they were exposed to serum, possibly because HN5 cells secrete high levels of EGF which promotes a high migration level of these cells also in serum-free conditions. Inherbin3 strongly inhibited serum-induced migration of A549 cells and basal migration of HN5 cells, whereas the scrambled Inherbin3 peptide Scr-Inherbin3 had no significant effects on cell migration (Fig. 6A and B).

For comparison, the effects of Cetuximab and PD153035 were also assessed. These inhibitors had no significant effect on cell migration in either HN5 or A549 cells. In summary, Inherbin3 functions as an effective inhibitor of cell migration in two ErbB1-expressing tumor cell lines, in which the ErbB1 inhibitors PD153035 and Cetuximab show no effect on cell migration.

To identify important amino acid residues for the inhibitory effect on cell migration, we analyzed the effect of a series of Inherbin3 derivatives, in which the amino acid sequence was systematically truncated from the N- and C-termini. All peptide derivatives were used in the same concentrations (11 μM), and the effect on A549 cell migration was determined for each peptide. As shown in Fig. 6C, truncation of Inherbin3 peptide from the N-terminus by two residues was enough to abrogate its inhibitory effect on cell migration. Moreover, peptides truncated from the C-terminus by two, four or six residues retained their inhibitory activity,

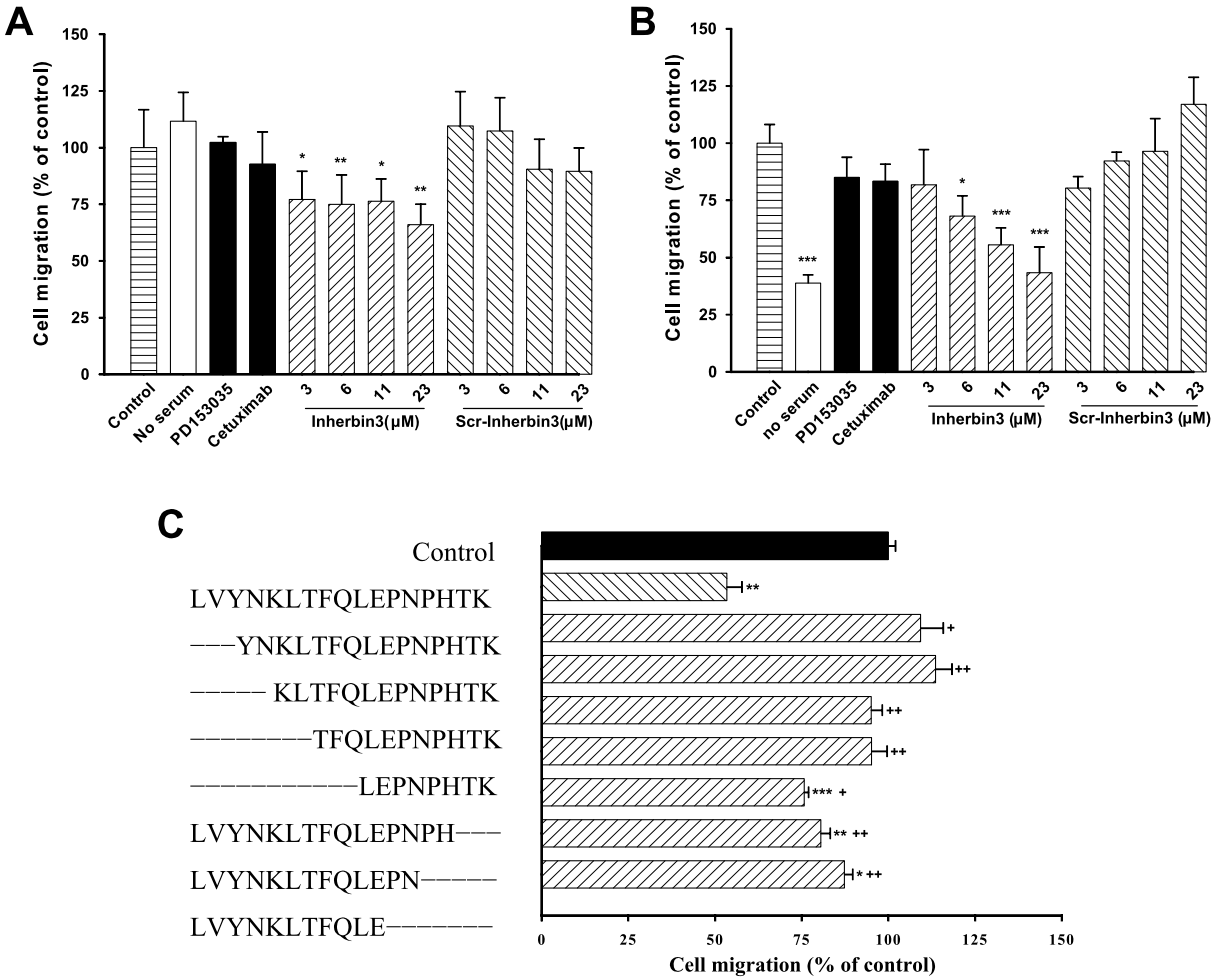

Fig. 6. Effect of Inherbin3 on HN5 and A549 cell migration. HN5 (A) or A549 (B and C) cells were seeded in serum-free medium containing Inherbin3 or scrambled Inherbin3 at the indicated concentrations, 100 nM PD153035, or 50 μg/ml Cetuximab. The concentration of Inherbin3 or truncated peptides from Inherbin3 in panel C was 11 μM. Cells were allowed to migrate for 24 h into the feeder tray containing medium supplemented with 10% serum (except in wells corresponding to the column "no serum" which contained serum-free medium in the feeder tray) and peptides and inhibitors at concentrations that were the same as in the corresponding migration chamber wells. Data are expressed as mean ± SEM of 4 independent experiments. $^{*}p < 0.05$, $^{**}p < 0.01$, $^{***}p < 0.001$, significant difference compared with untreated cells (control) (Student's paired t-test). $^{+}p < 0.05$, $^{++}p < 0.01$, significant difference compared with Inherbin3 (Student's paired t-test).

although they did not inhibit migration to the same low level as the full-length peptide.

3.5. *Inherbin3 inhibits in vivo tumor growth in a SCID mouse xenograft model using the human NSCLC A549 cell line*

To evaluate the potential of Inherbin3 to inhibit tumor growth *in vivo*, we next investigated the effect of subcutaneous administration of Inherbin3 on the growth of tumor xenografts of the A549 cell line grafted into immune-deficient SCID mice. Three independent experiments were performed with the same dose of Inherbin3 but different active control substances. Mice received a daily dose of 3 mg/kg Inherbin3 or scr-Inherbin3 or vehicle starting from day 13 after tumor inoculation, and tumor growth was monitored three times weekly for 5 weeks. For comparison, the effect of the general cytostatic drug Taxol (paclitaxel) administered intraperitoneally three times weekly, Erbitux (Cetuximab) administered intraperitoneally twice weekly, and Tarceva (erlotinib) administered orally daily starting on day 13 after tumor inoculation was also assessed. As shown in Fig. 7A and B, Inherbin3 significantly inhibited tumor growth

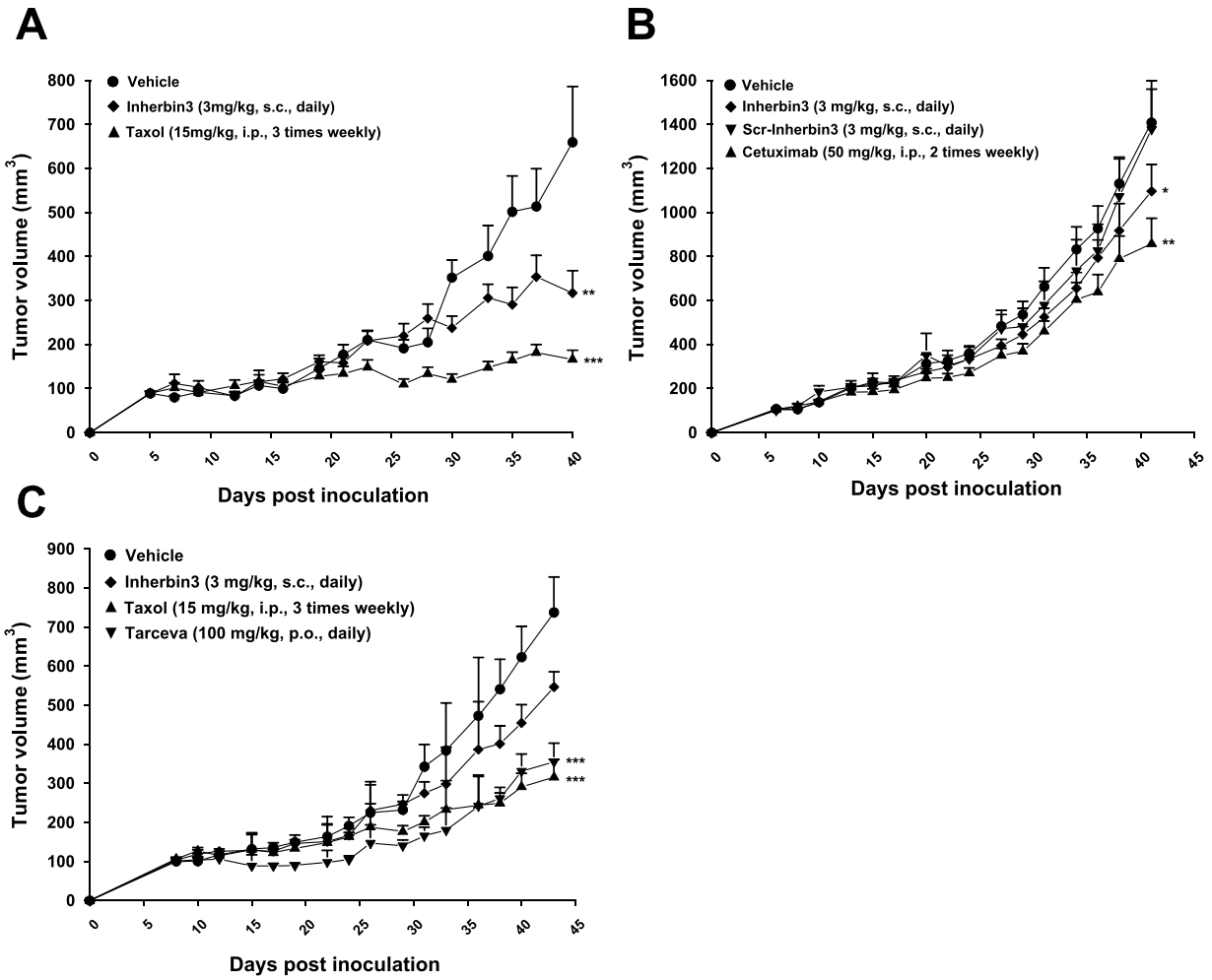

Fig. 7. Effect of Inherbin3 on *in vivo* tumor growth in a SCID mouse xenograft model using the NSCLC A549 cell line. (A) Eight to nine female SCID mice per treatment group were inoculated subcutaneously with A549 cells. Treatment with vehicle (sterile water), 3 mg/kg Inherbin3 or 15 mg/kg Taxol was initiated on day 13 after tumor inoculation. Inherbin3 and vehicle were administered subcutaneously daily, and Taxol was administered intraperitoneally three times weekly. (B) Eight female SCID mice per treatment group were inoculated subcutaneously with A549 cells. Treatment with vehicle (sterile water), 3 mg/kg Inherbin3, 3 mg/kg scr-Inherbin3 or 50 mg/kg Cetuximab was initiated on day 13 after tumor inoculation. Inherbin3, scr-Inherbin3 and vehicle were administered subcutaneously daily, and Cetuximab was administered intraperitoneally twice weekly. (C) Ten female SCID mice per treatment group were inoculated subcutaneously with A549 cells. Treatment with vehicle (MilliQ water), 3 mg/kg Inherbin3, 15 mg/kg Taxol or 100 mg/kg Tarceva was initiated on day 13 after tumor inoculation. Inherbin3 and vehicle were administered subcutaneously daily, Tarceva was administered orally daily, and Taxol was administered intraperitoneally three times weekly. Tumor size was monitored three times weekly and compared with untreated animals (vehicle). $^{*}p < 0.05$, $^{**}p < 0.01$, $^{***}p < 0.001$, compared with vehicle-treated control (one-way analysis of variance followed by a Newman–Keuls *post hoc* test).

in two experiments. The scrambled peptide had no effect, suggesting that the inhibitory effect of Inherbin3 was sequence-specific. In the third experiment, the effect of Inherbin3 did not reach statistical significance (Fig. 7C). Taxol, Tarceva and Cetuximab also significantly inhibited tumor growth. Compared with the tested dose of Inherbin3 (3 mg/kg), Taxol, Tarceva and Cetuximab showed a stronger tumor inhibitory effect with an earlier onset.

3.6. Inherbin3 induces cell apoptosis in a SCID mouse xenograft model with the human NSCLC A549 cell line

To evaluate the potential of Inherbin3 to induce tumor cell apoptosis, we investigated the effect of Inherbin3 on cell apoptosis in xenografts of the human NSCLC A549 cell line grafted into immune-deficient SCID mice from the first *in vivo* experiment, in which

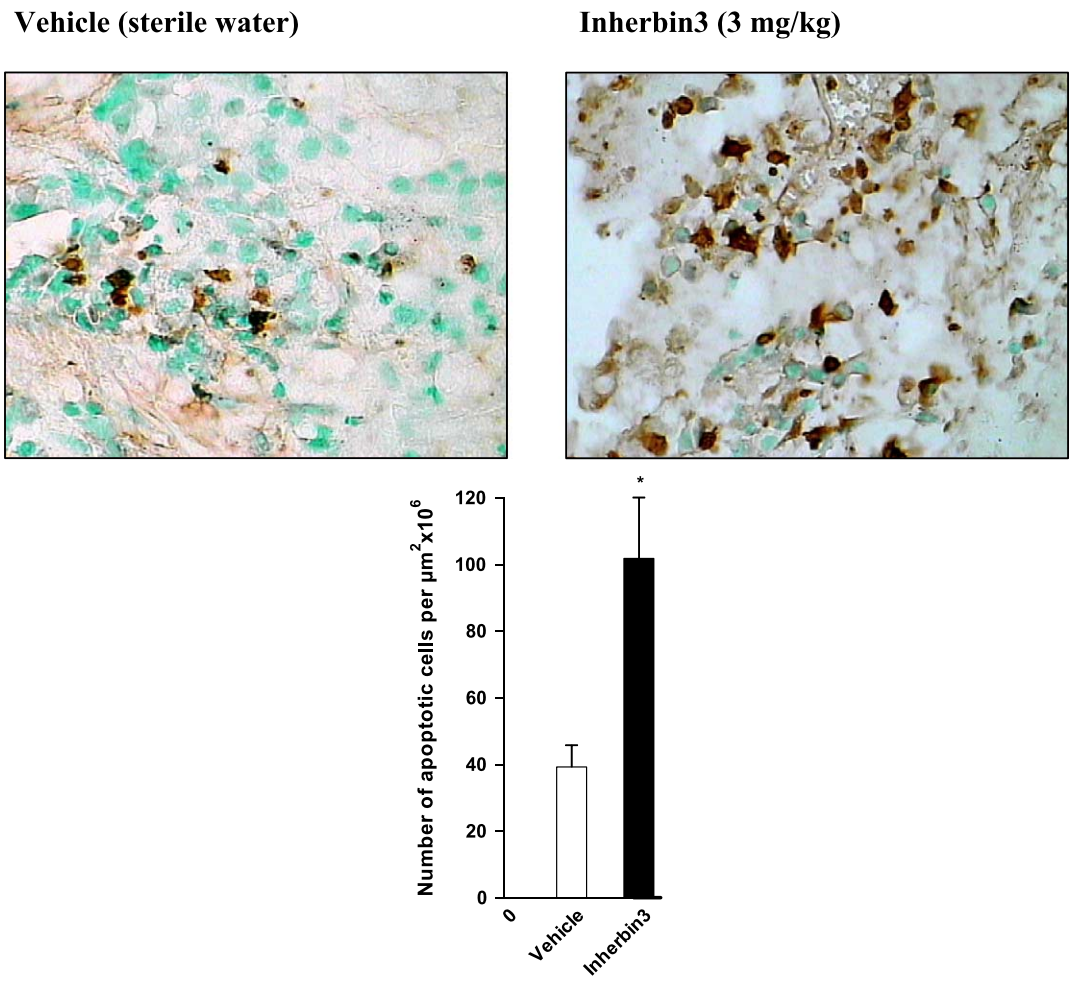

Fig. 8. Effect of Inherbin3 on cell apoptosis in a SCID mouse xenograft model with the NSCLC A549 cell line. Tumors from the groups treated with vehicle (sterile water) or 3 mg/kg Inherbin3 (experiment 1, shown in Fig. 7A) were analyzed. Three 10 μm-thick sections of each tumor were stained with TUNEL to visualize apoptotic cells. The number of TUNEL-positive cells was counted for each section. $^{*}p < 0.05$, compared with vehicle-treated tumors (control) (Student's paired t-test).

the peptide significantly inhibited tumor growth. As shown in Fig. 8, treatment with 3 mg/kg Inherbin3 resulted in an increase in cell apoptosis compared with the vehicle-treated animals.

4. Discussion

Dimerization is essential for ErbB receptor activity, although dimerization *per se* does not appear to be sufficient for ErbB receptor activation. Thus, several studies have demonstrated that ErbB receptors are found on the cell surface as preformed, inactive dimers [23,36]. These preformed dimers appear to be, at least for ErbB1, primarily stabilized by transmembrane and intracellular interactions, whereas the active, ligand-induced dimers are stabilized primarily by extracellular receptor–receptor interactions. The transition from the inactive dimeric state to the active dimeric conformation is probably driven by ligand-induced dimerization of the extracellular parts of the two receptor molecules in the dimer, mediated primarily by the so-called dimerization arm sequence in the second extracellular domain. This dimerization of the extracellular parts appears to be the critical event in receptor activation. On this basis, we hypothesized that peptides comprising the dimerization arm sequences of ErbB receptors might function as inhibitors of ligand-induced ErbB receptor homo- and heterodimerization, and thereby inhibitors of ErbB receptor signaling, by blocking the

sites in the second extracellular domain of the receptors, which in the absence of peptide would bind the dimerization arm of a dimerization partner. The data presented in this paper provide the first biochemical and biological characterization of one such peptide, termed Inherbin3, that comprises an amino acid sequence derived from the dimerization arm of ErbB3.

We first assessed the binding profile of the Inherbin3 peptide against the extracellular domains of the ErbB receptors. We found that Inherbin3 bound to the extracellular domains of all four ErbB receptors. The affinity constant measurements indicate that Inherbin3 probably has a potential to affect homo- and heterodimerization processes involving ErbB1, ErbB2 and ErbB3. Notably, our binding studies do not provide information about where in the extracellular part of the ErbB receptors the Inherbin3 peptide binds. Additionally, the binding studies do not reveal whether the peptide binds the same site in all four ErbB receptor extracellular parts. To prove that Inherbin3 actually binds to the intended site in domain II, which is responsible for binding of the dimerization arm of a dimerization partner, studies of Inherbin3 binding to individual ErbB receptor domains or to ErbB receptor deletion mutants lacking the relevant regions of domain II would be required. However, assuming that Inherbin3 actually mimics the ErbB3 dimerization arm, our binding results support the hypothesis that the dimerization arm of ErbB3 may be able to mediate homo- and heterodimerization of ErbB3 with each of the four ErbB receptors.

For characterization of the biological effects of the Inherbin3 peptide in tumor cells, we employed two ErbB1-expressing tumor cell lines that represent two tumor types (NSCLC and SCCHN) in which ErbB1 signaling is known to play an essential role in the development and progression of the disease, and in which inhibition of ErbB1 has proven to be a promising treatment strategy [1,29,39]. Our analysis of the biological effects of the Inherbin3 peptide reveals that the peptide is able to interfere with ErbB1 function in these tumor types.

When investigating the effects of Inherbin3 at the receptor level, we found that Inherbin3 was able to inhibit EGF-induced ErbB1 phosphorylation in both HN5 and A549 cells. We hypothesise that the ability of Inherbin3 to block ligand-induced ErbB1 activity is the result of the following mechanism of action: Inherbin3 binds, as intended in the peptide design, to the region in domain II of ErbB1, which in the absence of Inherbin3 would bind the dimerization arm of another ErbB1 molecule in an ErbB1 homodimer. In the absence of ligand, this region of domain II, together with the dimerization arm itself, is buried in the domain II/IV "tether" interface [10]. Upon ligand binding, this tether is broken, and the dimerization arm, as well as the region responsible for binding the dimerization arm of a dimerization partner (i.e., the region that we hypothesize will also bind the Inherbin3 peptide) are exposed [9]. Due to the dimeric nature of the Inherbin3 peptide employed in all cellular assays in this study, the peptide possibly binds two ErbB1 molecules simultaneously, thereby keeping the receptors in a sterically fixed position relative to each other, with the dimerization loop binding regions blocked, thereby hindering "proper" (i.e., which would result in receptor activation) dimerization of the receptors.

At the cellular level, we investigated the effect of Inherbin3 on two cellular responses known to be promoted by ErbB1 signaling: cell proliferation and cell migration [22,38,41,42]. Inherbin3 significantly inhibited the proliferation of ErbB1-overexpressing HN5 and A549 cells, but not Cos-7 cells expressing negligible amounts of ErbB1. The most pronounced growth inhibitory effect was seen in HN5 cells, indicating a selectivity of this effect for cell lines expressing high levels of ErbB1. For comparison, we tested the effect of two known ErbB1 inhibitors, the small-molecule ErbB1 kinase inhibitor PD153035 and the monoclonal antibody Cetuximab. These inhibitors strongly inhibited HN5 cell growth but had no significant effects on A549 cell growth, indicating that the effect of these inhibitors is even more selective for cell lines expressing high levels of ErbB1. Thus, our data suggest that Inherbin3 is able to inhibit the *in vitro* growth of different ErbB1-expressing tumor cell lines, including *in vitro* cell lines that are resistant to known ErbB1 inhibitors such as PD153035 and Cetuximab.

With regard to the effect of Inherbin3 on cell migration, we found that Inherbin3 functions as a strong inhibitor of the migration of both HN5 and A549 cells. In contrast, PD153035 and Cetuximab had no significant effect on the migration of either HN5 or A549 cells. Migration is essential for tumor growth as well as the ability of tumor cells to migrate into the circulatory system and into new tissues leading to metastasis [16]. Thus, the strong effects of Inherbin3 on tumor cell migration compared with the lack of effect of the ErbB1 inhibitors PD153035 and Cetuximab indicates the potential of Inherbin3 to function as a multifaceted inhibitor of tumor growth *in vivo* and in tumor types in which the effects of known ErbB1 inhibitors may not

be sufficient to significantly control expansion of the tumor.

The clear differences between the effects of Inherbin3 and the effects of the ErbB1 inhibitors PD153035 and Cetuximab is intriguing and suggests that Inherbin3 may not be a mere ErbB1 inhibitor, similar to PD153035 and Cetuximab, but may have additional mechanisms of actions. We speculate that Inherbin3 may act as an inhibitor not only of ErbB1 homodimerization, but also of the formation of other ErbB receptor homo- or heterodimers, a speculation that is supported by our finding that Inherbin3 is able to bind the extracellular parts of all four ErbB receptors. Because several ErbB receptors are often co-expressed in the same tumor, where they cooperatively contribute to the development and progression of the cancer [14], a peptide that binds to and interferes with the homo- and heterodimerization properties of several ErbB receptor family members might have an advantage over drugs that target a single ErbB receptor. Another possibility is that the difference between Inherbin3 and the other tested ErbB1 inhibitors lies in the magnitude of their inhibitory effect on the receptor. Whereas PD153035 and Cetuximab both confer full blockade of receptor activity, Inherbin3 functions as a partial inhibitor of EGF-induced ErbB1 phosphorylation. This partial inhibition of the receptor may have advantageous effects that are not yet fully understood, e.g. the induction of a low level of ErbB1 signaling may result in inhibition of cell migration. Moreover, the partial inhibition may also have disadvantageous effects, e.g. giving rise to development of resistance.

The last part of our characterization of the biological effects of Inherbin3 in tumor cells investigated the effect of Inherbin3 on tumor growth *in vivo*. On the basis of the effects of Inherbin3 on proliferation and migration of the A549 cell line, which in our *in vitro* characterization had proven resistant to the other ErbB1 inhibitors PD153035 and Cetuximab, we employed a xenograft model using tumors established from the NSCLC A549 cell line. The ErbB1 kinase inhibitor erlotinib (Tarceva) has been approved for the treatment of locally advanced or metastatic NSCLC after failure of at least one prior chemotherapy regimen [39]. The monoclonal anti-ErbB1 antibody Cetuximab (Erbitux) has shown promising effects against NSCLC in clinical trials [39]. However, although ErbB1 overexpression has been reported in 43–83% of NSCLC cases [29], the number of NSCLC patients who respond to Tarceva and Erbitux is much smaller, and the objective response rates are relatively low [8]. Thus, an urgent need exists for the development of alternative drugs against NSCLC.

Three independent *in vivo* tumor growth experiments were performed in the present study. In the first two experiments, Inherbin3 showed a promising tumor-inhibiting effect in this model, although the effect of Inherbin3 was not as pronounced as the effect of Taxol, a broadly acting tubulin-targeting cytotoxic compound that was used as an active control. The results should be viewed from the perspective that animals treated with Taxol showed significant signs of general toxicity of this compound (e.g., hair loss, body weight loss, reduced appetite, etc.), whereas Inherbin3-treated mice showed no signs of toxicity. In the third experiment, Inherbin3 showed a tendency toward inhibition of tumor growth, although the effect did not reach statistical significance in this experiment. After the end of the first *in vivo* study, the tumors were collected and analyzed for the amount of apoptotic tumor cells by means of a histochemical TUNEL assay. Inherbin3 significantly induced cell apoptosis compared with vehicle.

The growth-inhibiting effect of Inherbin3 in the A549 tumor xenograft model shows that Inherbin3 represents a potential peptide therapeutic against NSCLC. Our *in vitro* data, as well as other *in vitro* and *in vivo* studies [25,26,33], have demonstrated that the A549 cell line is either resistant or only moderately responsive to known ErbB1 inhibitors such as Cetuximab and Erlotinib. In contrast, in our *in vivo* studies, both Tarceva and Cetuximab exerted a significant tumor-inhibiting effect, which was stronger than the *in vivo* effect of Inherbin3. Thus, Inherbin3 showed ability to partially inhibit growth of A549 tumors *in vivo*, but the peptide effect was not optimal, indicating that further improvements in the design of the peptide are needed.

In conclusion, we demonstrated that a peptide constituting the dimerization arm sequence of ErbB3, the Inherbin3 peptide, bound to the extracellular parts of ErbB receptors and inhibited ErbB1 phosphorylation, cell proliferation and migration in ErbB1-expressing tumor cells. Interestingly, we demonstrated that the effects of Inherbin3 on ErbB1 receptor phosphorylation, tumor cell proliferation, and tumor cell migration differed significantly from the effects of two known ErbB1 inhibitors, PD153035 and Cetuximab. Furthermore, we showed that Inherbin3 was able to inhibit *in vivo* tumor growth in an NSCLC xenograft mouse model. These findings indicate that peptide-based targeting of ErbB receptor dimerization may be a promising novel therapeutic strategy against NSCLC and perhaps also SCCHN tumors.

Acknowledgements

Research was financially supported by grants from the Danish Research Councils, the European Union's 6th framework programme PROMEMORIA (LSHM-CT-2005-512012), Novo Nordisk Foundation, Carlsberg Foundation, Dagmar Marshalls Foundation, Fabrikant Einar Willumsens Mindelegat Foundation, Danish Cancer Research Foundation and Warwara Larsens Foundation.

References

[1] S.M. Ahmed and E.E. Cohen, Treatment of squamous cell carcinoma of the head and neck in the metastatic and refractory settings: advances in chemotherapy and the emergence of small molecule epidermal growth factor receptor kinase inhibitors, *Curr. Cancer Drug Targets* **7** (2007), 666–673.

[2] A. Berezov, J. Chen, Q. Liu, H.T. Zhang, M.I. Greene and R. Murali, Disabling receptor ensembles with rationally designed interface peptidomimetics, *J. Biol. Chem.* **277** (2002), 28330–28339.

[3] A. Berezov, H.T. Zhang, M.I. Greene and R. Murali, Disabling ErbB receptors with rationally designed exocyclic mimetics of antibodies: structure-function analysis, *J. Med. Chem.* **44** (2001), 2565–2574.

[4] S. Bouyain, P.A. Longo, S. Li, K.M. Ferguson and D.J. Leahy, The extracellular region of ErbB4 adopts a tethered conformation in the absence of ligand, *Proc. Natl. Acad. Sci. USA* **102** (2005), 15024–15029.

[5] A.W. Burgess, H.S. Cho, C. Eigenbrot et al., An open-and-shut case? Recent insights into the activation of EGF/ErbB receptors, *Mol. Cell* **12** (2003), 541–552.

[6] H.S. Cho and D.J. Leahy, Structure of the extracellular region of HER3 reveals an interdomain tether, *Science* **297** (2002), 1330–1333.

[7] H.S. Cho, K. Mason, K.X. Ramyar et al., Structure of the extracellular region of HER2 alone and in complex with the Herceptin Fab, *Nature* **421** (2003), 756–760.

[8] F. Ciardiello and G. Tortora, EGFR antagonists in cancer treatment, *N. Engl. J. Med.* **358** (2008), 1160–1174.

[9] K.M. Ferguson, Active and inactive conformations of the epidermal growth factor receptor, *Biochem. Soc. Trans.* **32** (2004), 742–745.

[10] K.M. Ferguson, M.B. Berger, J.M. Mendrola, H.S. Cho, D.J. Leahy and M.A. Lemmon, EGF activates its receptor by removing interactions that autoinhibit ectodomain dimerization, *Mol. Cell* **11** (2003), 507–517.

[11] T.P.J. Garrett, N.M. McKern, M. Lou et al., Crystal structure of a truncated epidermal growth factor receptor extracellular domain bound to transforming growth factor α, *Cell* **110** (2002), 763–773.

[12] T.P.J. Garrett, N.M. McKern, M. Lou et al., The crystal structure of a truncated ErbB2 ectodomain reveals an active conformation, poised to interact with other ErbB receptors, *Mol. Cell* **11** (2003), 495–505.

[13] P.M. Guy, J.V. Platko, L.C. Cantley, R.A. Cerione and K.L. Carraway 3rd, Insect cell-expressed p180erbB3 possesses an impaired tyrosine kinase activity, *Proc. Natl. Acad. Sci. USA* **91** (1994), 8132–8136.

[14] N.E. Hynes and G. MacDonald, ErbB receptors and signaling pathways in cancer, *Curr. Opin. Cell. Biol.* **21** (2009), 177–184.

[15] R.N. Jorissen, F. Walker, N. Pouliot, T.P. Garrett, C.W. Ward and A.W. Burgess, Epidermal growth factor receptor: mechanisms of activation and signalling, *Exp. Cell Res.* **284** (2003), 31–53.

[16] M. Kirsch, G. Schackert and P.M. Black, Metastasis and angiogenesis, *Cancer Treat. Res.* **117** (2004), 285–304.

[17] L.N. Klapper, S. Glathe, N. Vaisman, N.E. Hynes, G.C. Andrews, M. Sela and Y. Yarden, The ErbB-2/HER2 oncoprotein of human carcinomas may function solely as a shared coreceptor for multiple stroma-derived growth factors, *Proc. Natl. Acad. Sci. USA* **96** (1999), 4995–5000.

[18] J. Knight, B.A. Gusterson, G. Cowley and P. Monaghan, Differentiation of normal and malignant human squamous epithelium *in vivo* and *in vitro*: a morphologic study, *Ultrastruct. Pathol.* **7** (1984), 133–141.

[19] Z. Li, Y. Mei, X. Liu and M. Zhou, Neuregulin-1 only induces trans-phosphorylation between ErbB receptor heterodimer partners, *Cell. Signal.* **19** (2007), 466–471.

[20] M.D. Marmor, K.B. Skaria and Y. Yarden, Signal transduction and oncogenesis by ErbB/HER receptors, *Int. J. Radiat. Oncol. Biol. Phys.* **58** (2004), 903–913.

[21] D. Mattoon, P. Klein, M.A. Lemmon, I. Lax and J. Schlessinger, The tethered configuration of the EGF receptor extracellular domain exerts only a limited control of receptor function, *Proc. Natl. Acad. Sci. USA* **101** (2004), 923–928.

[22] G.T. Merlino, Epidermal growth factor receptor regulation and function, *Semin. Cancer Biol.* **1** (1990), 277–284.

[23] T. Moriki, H. Maruyama and I.N. Maruyama, Activation of preformed EGF receptor dimers by ligand-induced rotation of the transmembrane domain, *J. Mol. Biol.* **311** (2001), 1011–1026.

[24] T. Nakamura, H. Takasugi, T. Aizawa et al., Peptide mimics of epidermal growth factor (EGF) with antagonistic activity, *J. Biotechnol.* **116** (2005), 211–219.

[25] G.N. Naumov, M.B. Nilsson, T. Cascone et al., Combined vascular endothelial growth factor receptor and epidermal growth factor receptor (EGFR) blockade inhibits tumor growth in xenograft models of EGFR inhibitor resistance, *Clin. Cancer Res.* **15** (2009), 3484–3494.

[26] D.A. Nikolova, I.A. Asangani, L.D. Nelson et al., Cetuximab attenuates metastasis and u-PAR expression in non-small cell lung cancer: u-PAR and E-cadherin are novel biomarkers of cetuximab sensitivity, *Cancer Res.* **69** (2009), 2461–2470.

[27] N. Normanno, C. Bianco, L. Strizzi et al., The ErbB receptors and their ligands in cancer: an overview, *Curr. Drug Targets* **6** (2005), 243–257.

[28] H. Ogiso, R. Ishitani, O. Nureki et al., Crystal structure of the complex of human epidermal growth factor and receptor extracellular domains, *Cell* **110** (2002), 775–787.

[29] G.S. Papaetis, C. Roussos and K.N. Syrigos, Targeted therapies for non-small cell lung cancer, *Curr. Pharm. Des.* **13** (2007), 2810–2831.

[30] B.W. Park, H.T. Zhang, C. Wu et al., Rationally designed anti-HER2/neu peptide mimetic disables P185$^{HER2/neu}$ tyrosine kinases *in vitro* and *in vivo*, *Nat. Biotechnol.* **18** (2000), 194–198.

[31] J. Schlessinger, Ligand-induced, receptor-mediated dimerization and activation of EGF receptor, *Cell* **110** (2002), 669–672.

[32] W.X. Schulze, L. Deng and M. Mann, Phosphotyrosine interactome of the ErbB-receptor kinase family, *Mol. Syst. Biol.* **1** (2005), 2005.0008.

[33] W. Shao, S. Zhao, Z. Liu et al., Inhibition of human tumor xenograft growth in nude mice by a conjugate of monoclonal antibody LA22 to epidermal growth factor receptor with antitumor antibiotics mitomycin C, *Biochem. Biophys. Res. Commun.* **349** (2006), 816–824.

[34] L. Sun and J.A. Gardella Jr., The solid state oxidation of methionine containing peptide: a preliminary study using time of flight secondary ion mass spectrometry, *Pharm. Res.* **17** (2000), 859–862.

[35] Z. Tang, S. Jiang, R. Du et al., Distruption of the EGFR E884-R958 ion pair conserved in the human kinome differentially alters signaling and inhibitor sensitivity, *Oncogene* **28** (2009), 518–533.

[36] R.H. Tao and I.N. Maruyama, All EGF (ErbB) receptors have preformed homo- and heterodimeric structures in living cells, *J. Cell. Sci.* **121** (2008), 3207–3217.

[37] F. Walker, S.G. Orchard, R.N. Jorissen et al., CR1/CR2 interactions modulate the functions of the cell surface epidermal growth factor receptor, *J. Biol. Chem.* **279** (2004), 22387–22398.

[38] A. Wells, J. Kassis, J. Solava, T. Turner and D.A. Lauffenburger, Growth factor-induced cell motility in tumor invasion, *Acta Oncol.* **41** (2002), 124–130.

[39] P. Wheatley-Price and F.A. Shepherd, Epidermal growth factor receptor inhibitors in the treatment of lung cancer: reality and hopes, *Curr. Opin. Oncol.* **20** (2008), 162–175.

[40] K.J. Wilson, J.L. Gilmore, J. Foley, M.A. Lemmon and D.J. Riese 2nd, Functional selectivity of EGF family peptide growth factors: implications for cancer, *Pharmacol. Ther.* **122** (2009), 1–8.

[41] C. Xue, J. Wyckoff, F. Liang et al., Epidermal growth factor receptor overexpression results in increased tumor cell motility *in vivo* coordinately with enhanced intravasation and metastasis, *Cancer Res.* **66** (2006), 192–197.

[42] Y. Yarden and M.X. Sliwkowski, Untangling the ErbB signalling network, *Nat. Rev. Mol. Cell Biol.* **2** (2001), 127–137.